

An optical 3D sound intensity and energy density probe

Cazzolato, B.S. (1), Halim, D. (1), Petersen, D. (1), Kahana, Y. (2) and Kots, A. (2)

(1) School of Mechanical Engineering, The University of Adelaide, SA, 5005, Australia

(2) Phone-Or Ltd, 17 Hataasia St., or-Yehuda 60212, Israel

ABSTRACT

In this paper, an optical sensor capable of measuring pressure and the three orthogonal particle velocities at a point is presented. This sensor can be used to measure three-dimensional sound intensity or energy density in the presence of strong electro-magnetic and radio-frequency fields. The benefits of the sensor compared to traditional p-p intensity probes is discussed, as well as the design, construction and performance of the sensor. It will be seen that this new type of sensor has many advantages compared to traditional sensors.

INTRODUCTION

Motivated by the desire to be able to measure sound in strong electro-magnetic fields, like those found near electrical transformers (Li et al., 2002) and modern medical imaging systems such as MRI and CT (Kahana et al., 2004), the Active Noise and Vibration Control Group at the University of Adelaide commissioned PHONE-OR to design and build an entirely optical sensing system capable of measuring both sound intensity and energy density in 3 axes (Kahana, 2004). The device consists of one omni-directional pressure sensing element and three orthogonally mounted pressure gradient microphones used to provide an estimate of the particle velocity.

In Section ‘‘Sensing Sound Intensity / Energy Density’’ previous sensor arrangements for measuring sound intensity and energy density are discussed along with the limitations of these approaches. The details of the operation of the PHONE-OR optical microphones are discussed in detail in Section ‘‘The Phone-Or Optical Microphone’’. Finally, the construction and test results of the 3D optical sensor are presented in Section ‘‘The Optical Three-Dimensional Sensor’’.

SENSING SOUND INTENSITY / ENERGY DENSITY

There are a great number of publications related to the measurement of sound intensity and its less commonly used sibling energy density. The text titled Sound Intensity by Fahy (1995) provides a definitive reference on sound intensity. The work by Elko (1984, 1985), Schumacher and Hixson (1983) and Schumacher, 1984) are good sources of information on energy density. The material presented below is only a very brief summary of these two measures, intended to highlight problems with existing measurement methods.

In order to measure either sound intensity or energy density, an estimate of the pressure (p) and total particle velocity (v) at a point is required. The complex sound intensity is obtained by the product of the complex pressure and complex particle velocity, and is given by

$$I = \frac{1}{2} \Re \{ p \times v^* \} \quad (1)$$

$$J = \frac{1}{2} \Im \{ p \times v^* \} \quad (2)$$

where I is the real part of the complex intensity known as the active intensity, and J is the imaginary part known as the reactive intensity.

Sound energy density is obtained from the sum of the acoustic potential energy density and the acoustic kinetic energy density, and can be expressed as

$$ED(t) = \frac{p^2(t)}{2\rho_0 c_0^2} + \frac{\rho_0 v^2(t)}{2} \quad (3)$$

where ρ_0 is the density of the fluid and c_0 is the speed of sound in the fluid.

In most commercial systems for measuring the sound intensity and energy density, the pressure and velocity estimates are obtained using two closely spaced phase-matched pressure microphones (Fahy, 1995), known as the p-p principle. The pressure estimate is taken at the point midway between the two elements, viz

$$p(t) = \frac{p_1(t) + p_2(t)}{2} \quad (4)$$

and the velocity estimate may be approximated by the finite difference

$$v(t) = \frac{1}{\rho_0 h} \int_{-\infty}^t (p_1(\tau) - p_2(\tau)) d\tau \quad (5)$$

where p_1 and p_2 are the pressure estimates at the two microphone locations and h is the microphone spacing.

The finite difference approximation limits the bandwidth of conventional p-p sensors. The upper bound is set by the spatial Nyquist limit, with $kh < 1$ for accurate estimates, where k is the acoustic wavenumber. The lower frequency bound is predominantly limited by phase mismatches between the microphone elements but sensitivity mismatches, spatial positioning errors and random errors arising from poor coherence may also limit the response. Since the phase mismatch of microphones, including amplification, is typically in the order of 1° , then requiring a true phase difference of at least twice the mismatch bounds the lower operational limit to $kh > 2^\circ \pi / 180^\circ \approx 1/30 \approx 2^{-5}$ for accurate sensing. This means that even for the best phase matched

microphones, the operational bandwidth is in the order of 5 octaves.

The constraints discussed above also place limits on the size of the sensor, with measurements at the low frequency limit of human hearing requiring spacings of 100mm-200mm. Once one adds the microphone housing, the sensor can become very large indeed.

With such constraints, alternatives to the p-p technique have been investigated such as the p-v technique. This involves sensors directly capable of measuring velocity. Early velocity microphones tended to lack robustness and suffered from a poor dynamic range, and along with poor phase response meant this approach was even less attractive than the p-p technique. Recently the p-v MEMS based μ flown sound intensity probe (de Bree, 1997, 1998; de Bree et al., 1999a,b) became commercially available and does not suffer from all the problems early p-v sensors did. Unfortunately, this sensor still exhibits a complex sensitivity curve on the velocity channel(s) that must be compensated for. In addition, the cost of a 3D μ flown is in the order of AUD\$20k which is prohibitive for most applications, in particular active noise control systems.

Consequently, there is a need for an alternative technology that combines the benefits of the MEMS based p-v technique but does not require sensitivity equalisation and is less expensive than systems like the μ flown. The following two sections describe a system that meets these needs and also has additional advantages that no other system currently has.

THE PHONE-OR OPTICAL MICROPHONE

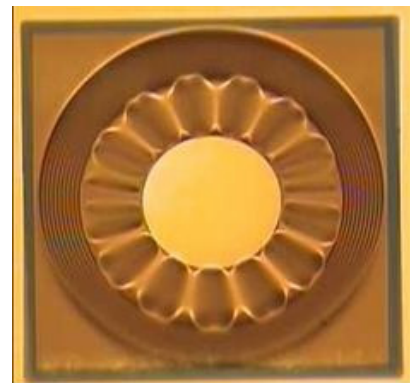
Margins and organisation of the paper

PHONE-OR's Fibre Optical Microphone (FOM) is based on Micro-Electro-Mechanical-Systems (MEMS) technology. A photograph showing the main microphone components is shown in Figure 1(a), with a SEM image of the pressure sensitive membrane shown in Figure 1(b). The circular and radial corrugations in the membrane are used to increase the pressure sensitivity of the membrane while maintaining elasticity and linearity. The dot in the centre of the membrane is a gold coating and serves as a reflective surface for the light. The omnidirectional microphone has a single vent in the housing, whereas the pressure gradient sensor is vented from both sides (Kahana et al., 2003).

The principle of operation is shown in Figure 2. Light emitted by a LED travels along an optical fibre to the optical head, which in turns beams light on the MEMS membrane. Sound causes the membrane to vibrate, thereby changing the intensity of the light reflected off the membrane into the photo-detector via a second optical fibre. The intensity modulated light is converted into an electrical signal through simple electronics.



(a) Microphone Components



(b) SEM image of the membrane

Figure 1. PHONE-OR Fibre Optical Microphone

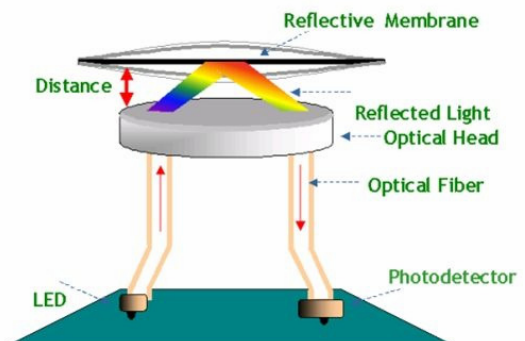
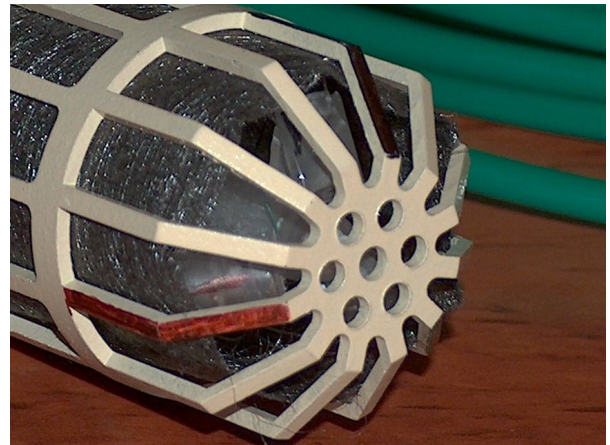


Figure 2. Principle of operation for the PHONE-OR Fibre Optical Microphone

The benefits of this technology include:

- **Pressure Gradient Accuracy:** The membrane characteristics, its construction, and assembly in the optical head ensures high accuracy of symmetry for the front and rear impinging acoustical signals. Since no external forces or loads act on the membrane, the “figure of eight” polarity is maintained throughout the frequency bandwidth.
- **EMI/RF Immunity:** The FOM uses modulation of coherent light scattered off a thin membrane to measure sound as opposed to conventional microphones including condenser, electret and dynamic microphones which rely on electronic circuits that contain capacitors (condenser/electret) or coils (dynamic). Consequently, these optical microphones are not affected by electrical, magnetic or electrostatic interference.

- **Bandwidth:** The FOM has an extremely high bandwidth for both pressure and pressure gradient elements, typically from 1Hz to 10kHz. The application here has had the bandwidth reduced from 10Hz to 4kHz in order to minimise the self-noise.
- **Dynamic Range:** The dynamic range of the FOM is at least 85dB. Maximum SPL is 130dB.
- **Signal to Noise Ratio (SNR):** The microphones have a high signal to noise ratio, typically in the order of 70dB.
- **Total Harmonic Distortion (THD):** The THD of the FOM is less than 1% at 94dBre20µPa over the entire frequency bandwidth.
- **Sensitivity:** The nominal sensitivity of the FOM is 100mV/Pa for the pressure microphones and 1.94 mV/(Pa/m) for the pressure gradient microphones.



(a) Sensor head

THE OPTICAL THREE-DIMENSIONAL SENSOR

Construction and Specifications

The optical 3D sensor (Figure 3) is comprised of a single omni-directional pressure microphone (yellow channel) and three pressure gradient microphones (black, red and green channels corresponding to x , y and z axes) mounted orthogonally in an acoustically transparent sensor head. The sensor head has an outer diameter of 36mm and a length of 53mm. The fibre optical cable is 10m in length, and can be easily extended to hundreds of metres with little loss in sensitivity. The electro-optical unit provides input and output connectors for the four pairs of microphones and the output is received via the BNC connectors.

The nominal frequency range of the transducer is between 10 Hz and 4 kHz with ± 2 dB variations (Kahana, 2004). It has a dynamic range of 85 dB with 3.5 Vrms maximum output level.

Testing and Results

The calibration tests were performed in an anechoic chamber at the University of Adelaide. All signal processing was conducted using a Brüel & Kjær PULSE system signal analyser. The bandwidth was 6.4 KHz, with 800 frequency bins in the FFT and 8 Hz bin-width.

Testing of pressure element

The PHONE-OR omni-directional pressure sensor was calibrated against a 0.25" Brüel & Kjær (B&K) microphone from a B&K Sound Intensity probe Type 3519. For this particular test, both sensors were placed back-to-back at a distance of about 2m from the sound source (a loudspeaker). Tests were repeated where the sound source was placed at both the front and the back of the sensors, i.e. forward and backward wave tests respectively. These two measurements were then averaged to remove any bias associated with sensor misalignment between the B&K microphone and the PHONE-OR omni-directional sensor.

The nominal pressure sensitivity used for the omni-directional element was 100 mV/Pa. This value has been used when plotting the results. The actual sensitivity of the PHONE-OR pressure element was found to be 112 mV/Pa.

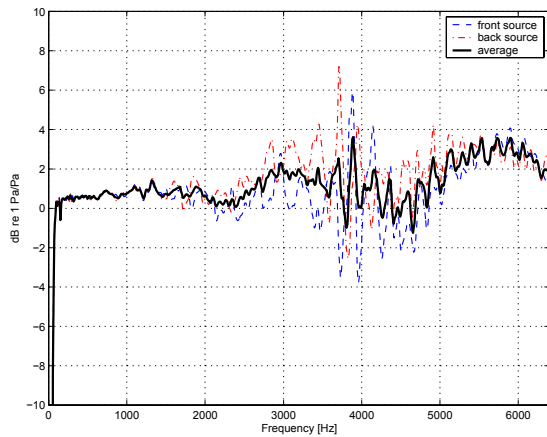


(b) Sensor head and electro-optical unit

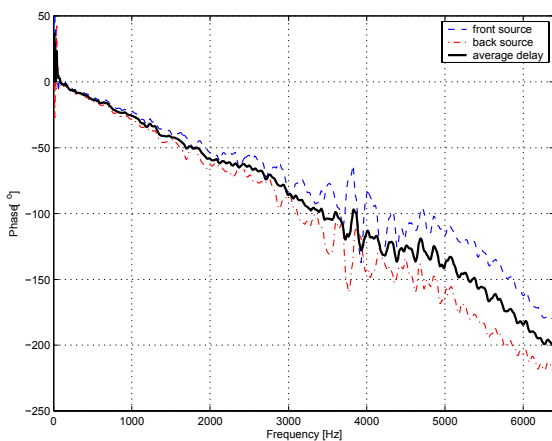
Figure 3. PHONE-OR 3D sensor (Kahana, 2004). Figure (a) shows the head. Figure (b) shows the head in the foreground and the electro-optical unit in the background. The acoustically transparent housing includes an omni-directional microphone, with its membrane orientated parallel to the housing tip. The three orthogonally arranged pressure gradient microphones are orientated at an angle of $35.26^\circ = \arctan(\sqrt{2})/2$ to the axis of symmetry to minimise the dimensions of the housing. The markers red, black and green indicate the axis for each sensor.

Figure 4 shows the frequency response between the B&K microphone and the PHONE-OR omni-directional pressure sensor. The magnitude results (Figure 4a) show that there is a small bias in the gain of approximately 1dB of the PHONE-OR sensor. The measurements from both sensors are relatively similar, particularly for frequencies between 80 Hz and 2.8 kHz (with less than 3 dB variation). The poor correlation at low frequencies is due to poor coherence resulting from low sound pressure levels. The high frequency variation is predominantly due to diffraction and scattering off both sensors and the mesh floor on which the equipment was suspended, and is commonly seen in this type of measurement (Steyer, 1984).

It can be seen that the “average” phase delay of the transducer is almost linear between 100Hz and 4kHz, with an equivalent “group” delay of 75 µs. The increasing phase lag after 4kHz is due to filtering aimed at reducing the self-noise.



(a) Magnitude



(b) Phase

Figure 4. Frequency response of back-to-back test between the PHONE-OR pressure element and the B&K microphone.

Testing of pressure gradient elements

The three PHONE-OR pressure gradient sensors were calibrated against a B&K Type 3519 Sound Intensity probe with two 0.25" phase-matched microphones and a 11mm spacer. With such a sensor spacing the results can be considered accurate from 250Hz to 5kHz. All tests were conducted in the far field of the noise source inside the anechoic chamber.

The pressure gradient measurements from the sound intensity and PHONE-OR probes were also compared to the pressure gradient estimation assuming a far-field condition. In this case, the pressure p in the far-field of an acoustic source is related to the particle velocity v by

$$\frac{p}{v} = \rho_0 c_0 \tag{6}$$

where $\rho_0 = 1.2\text{kg/m}^3$ and $c_0 = 343\text{m/s}$ are the air density and speed of sound respectively. The particle velocity is related to the pressure gradient by

$$j\omega v = -\frac{1}{\rho_0} \frac{\partial p}{\partial x} \tag{7}$$

By substituting Equation (6) into (7), the far-field pressure gradient may be estimated using the measured pressure, and is given by:

$$\frac{\partial p}{\partial x} = -\frac{j\omega p}{c_0} \tag{8}$$

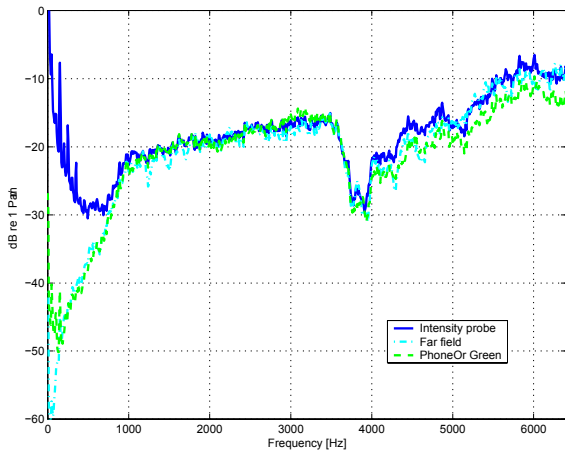
The nominal sensitivity of the pressure gradient elements provided by the PHONE-OR specifications (Kahana, 2004) is 35.5 mV/Pa, for the condition of 1" distance from the sound source, with the sensor facing the source at 1 kHz and 1 Pa. This form of specification is quite typical of gradient microphones used in audio applications. It can be shown that for the pressure gradient element which has an aperture separation of $\Delta x = 8.7\text{mm}$, the actual PHONE-OR pressure gradient sensitivity (Halim et al., 2004) is $(35.5\text{mV/Pa}) / (18.3\text{Pa/m}) = 1.94\text{mV}/(\text{Pa}\cdot\text{m})$. This value has been used throughout the following plots.

Figure 5 shows a typical pressure gradient auto-spectra measurement (for the green channel). The PHONE-OR measurements are compared to the gradient estimates obtained from the B&K sound intensity probe and from the far-field assumption using Equation (8). The results show that all three different methods of measurements are relatively similar up to 6.4 kHz, except for the B&K intensity probe measurement below 500 Hz. This discrepancy is caused by the low-frequency limitation of the small spacer used to separate the microphones in the intensity probe and illustrates the problems associated with using the pressure difference between two microphones to measure pressure gradient.

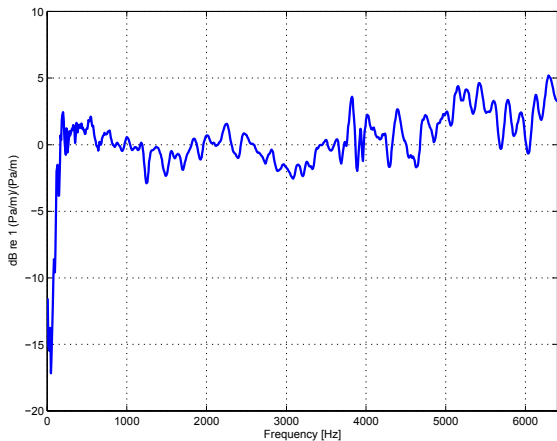
Typical frequency responses of the pressure gradient estimates are illustrated in Figure 6. The frequency responses are between measurements from the PHONE-OR (black channel) and far-field assumption, and also between the estimate from the sound intensity probe and the far field assumption. Between 160 Hz and 4 kHz, the PHONE-OR measurements are within 3 dB of the measurements using the far-field assumption. The low frequency measurements are compromised by low coherence due to low sound pressure levels.

It is interesting to see that the frequency response of the pressure gradient estimate from the sound intensity probe is flat down to 150Hz, unlike the auto-spectra from the probe shown in Figure 5. It suggests that the auto-spectra from the probe is corrupted by uncorrelated noise between the pressure element channels in the probe at low frequencies, arising from the low sound pressure levels and low phase difference (due to the low wavelength to microphone separation distance). This highlights one of the problems with using the p-p technique employed by most sound intensity transduction systems.

The phase delays associated with the PHONE-OR amplifier can be seen from the results, where the average group delay of the electronics for the gradient channel is 70 μs , which is (almost) the same as the group delay for the omni-directional element. This is important when calculating sound intensity, since any phase error between the pressure element and velocity elements will result in an error in the reactive and active intensity estimates. It is believed that the slight difference in group-delays between channels is simply due to experimental error, since the amplifying circuits were the same for all channels. The importance of phase errors between the pressure and particle velocity estimates is not an issue for sound energy density.

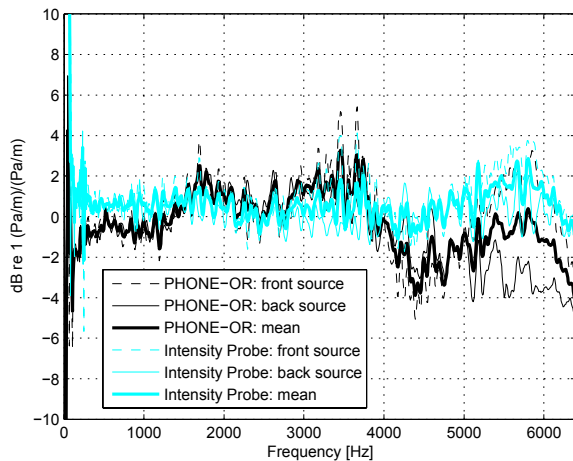


(a) Pressure gradient auto-spectra

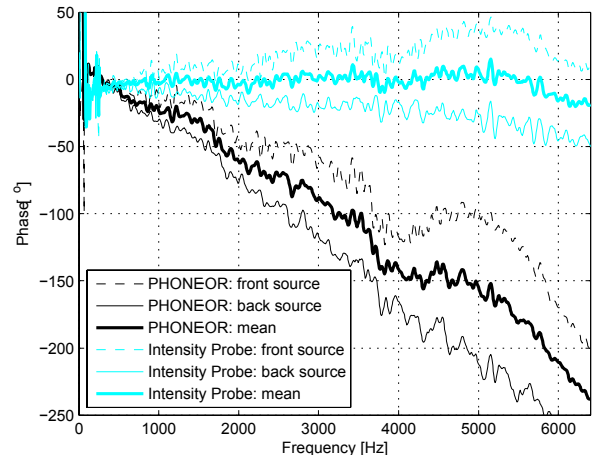


(b) Difference between pressure gradient estimates using the PHONE-OR and far-field auto-spectra

Figure 5. Auto-spectra of pressure gradient estimates: PHONE-OR pressure gradient channel, B&K sound intensity probe and far-field assumption.



(a) Magnitude

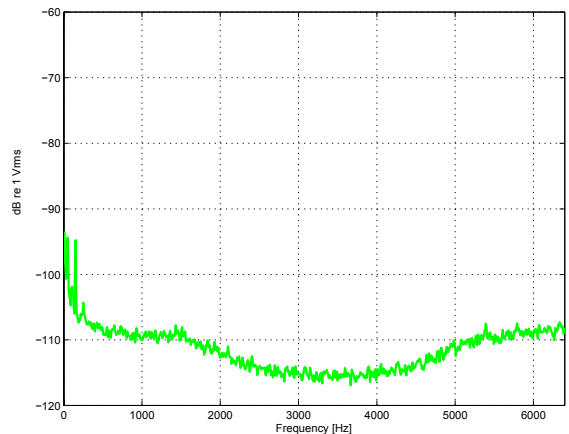


(b) Phase

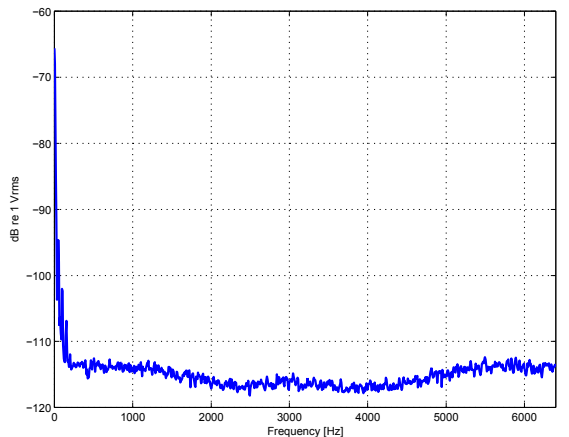
Figure 6. Frequency response function between the PHONE-OR (black) pressure gradient channel, the gradient estimate from the sound intensity probe and the far-field estimate.

Self-noise level tests

Finally, the self-noise for each of the channels were measured. Figure 7 shows the self-noise level of the PHONE-OR probe up to 6.4 kHz for the omni-directional element and the (green) pressure gradient element. The noise levels are due to 50 Hz harmonics. The total self-noise levels for all the microphones in the bandwidth displayed is approximately 0.5mVrms.



(a) Omni-directional



(b) Green pressure gradient

Figure 7. Auto-spectra of self-noise level for PHONE-OR omni-directional and (green) pressure gradient channel.

CONCLUSIONS

An optical sensor capable of measuring sound intensity and energy density has been built and tested. The sensor has a bandwidth of almost 9 octaves from 10Hz to 4kHz, compared to approximately 5 octaves for conventional dual microphone based sound intensity probes. It has a dynamic range of 80 dB, and a very low self-noise level of 0.5mVrms. Calibration of the device showed a flat frequency response of ± 2 dB over the dynamic range. The optical gradient sensor is considerably smaller in size than conventional p-p sound intensity probes for the same lower frequency limit. The test results demonstrate that the PHONE-OR optical 3D sensor is suitable for active noise control applications.

ACKNOWLEDGMENTS

The authors gratefully acknowledge the financial support for this work provided by the Australian Research Council.

REFERENCES

- de Bree, H.-E. 1997, *The Microflown*, PhD thesis, University of Twente.
- de Bree, H.-E. 1998, *The microflown: A true particle velocity microphone; Sound intensity application*, NAG Journal.
- de Bree, H.-E., Druyvesteyn, W.F., Berenschot, E. and Elwenspoek, M. 1999a, *Three dimensional sound intensity measurements using microflown particle velocity sensors*. In MEMs '99, Orlando.
- de Bree, H.-E., Druyvesteyn, W.F. and Elwenspoek, M. 1999b, *Realisation and calibration of a novel half inch P-U sound intensity probe*. In 106th AES Conference, Munich.
- Elko, G. 1984, *Frequency domain estimation of the complex acoustic intensity and acoustic energy density*, PhD thesis, Pennsylvania State University.
- Elko, G.W. 1985, *Simultaneous measurement of the complex acoustic intensity and the acoustic energy density*, Proceedings of the 2nd International Congress on Acoustic Intensity, pages 69-78.
- Fahy, F. 1995, *Sound Intensity*, E&FN Spon, London, 2nd edition.
- Halim, D., Petersen, D. and Cazzolato, B.S. 2004, *The phone-or 3d optical energy density probe: Calibration test report of the modified/re-calibrated probe*, Test report, The University of Adelaide.
- Kahana, Y. 2004, *3D sound field optical microphone system for EMI/RFI environments*, User Manual, Phone-Or.
- Kahana, Y., Kots, A., Mican, S., Chambers, J. and Bullock, D. 2004, *Optoacoustical ear defenders with active noise reduction in and MRI communication system*, In Proceedings of Active 04.
- Kahana, Y., Paritsky, A., Kots, A. and Mican, S. 2003, *Recent advances in optical microphone technology*, In Proceedings of Inter-Noise 2003.
- Li, X., Qiu, X., Hansen, C.H. and Ai, Y. 2002, *Active control of sound radiation from a small transformer using near field sensing*, International Journal of Acoustics and Vibration, 7(2).
- Schumacher, M. 1984, *A transducer and processing system for acoustic energy density*, Master's thesis, The University of Texas at Austin.
- Schumacher, M. and Hixson, E.L. 1983, *A transducer and processing system to measure total acoustic energy density*, Journal of the Acoustical Society of America, 74(S1):S62.
- Steyer, G.C. 1984, *Spectral methods for the estimation of acoustic intensity, energy density, and surface velocity using a multimicrophone probe*, PhD thesis, The Ohio State University.